

Benefits and limitations of a new hydraulic performance model

Fabian C. Weigend  · Edward Gray  ·
Oliver Obst  · Jason Siegler 

Abstract

Purpose Performance models are important tools for coaches and athletes to optimise competition outcomes or training schedules. A recently published hydraulic performance model has been reported to outperform established work-balance models in predicting recovery during intermittent exercise. The new hydraulic model was optimised to predict exercise recovery dynamics. In this work, we hypothesised that the benefits of the model come at the cost of inaccurate predictions of metabolic responses to exercise such as oxygen uptake (\dot{V}_{O_2}).

Methods Hydraulic model predictions were compared to breath-by-breath \dot{V}_{O_2} data from 25 constant high-intensity exercise tests of 5 participants (age 32 ± 7.8 years, weight 73.6 ± 5.81 kg, $\dot{V}_{O_{2\max}}$ 3.59 ± 0.62 L/min). Each test was performed to volitional exhaustion on a cycle ergometer with a duration between 2 and 12 min. The comparison focuses on the onset of \dot{V}_{O_2} kinetics.

Results On average, the hydraulic model predicted peak \dot{V}_{O_2} during exercise 216 ± 113 s earlier than observed in the data. The new hydraulic model also did not predict the so-called \dot{V}_{O_2} slow component and made the unrealistic assumption that there is no \dot{V}_{O_2} at the onset of exercise.

Conclusion While the new hydraulic model may be a powerful tool for predicting energy recovery, it should not be used to predict metabolic responses during high-intensity exercise. The present study contributes towards a more holistic picture

Fabian C. Weigend
School of Computer, Data and Mathematical Sciences and School of Health Sciences
Western Sydney University, Sydney, Australia
E-mail: Fabian.Weigend@westernsydney.edu.au

Edward Gray
School of Health Sciences
Western Sydney University, Sydney, Australia

Oliver Obst
School of Computer, Data and Mathematical Sciences
Western Sydney University, Sydney, Australia

Jason Siegler
College of Health Solutions
Arizona State University, Phoenix, USA

of the benefits and limitations of the new hydraulic model. Data and code are published as open source.

Keywords Performance Modelling · Bioenergetic Modelling · Hydraulic Performance Model · Oxygen Uptake Prediction

Abbreviations

CP	critical power
W'	finite energy reserve for work above critical power
W' balance	work-balance model
TTE	time to exhaustion
SEE	standard error of estimation
LAT	lactate threshold (moderate-heavy boundary)
\dot{V}_{O_2}	oxygen uptake
$\dot{V}_{O_2\max}$	maximal oxygen uptake
$\dot{V}_{O_2\text{peak}}$	peak oxygen uptake during a single test
P_{peak}	peak power output
M-M model	Margaria-Morton model
M-M-S model	Margaria-Morton-Sunström model
O	oxidative or aerobic energy source
$A_n A$	anaerobic alactic energy source
$A_n L$	anaerobic lactic energy source
T	tap at the bottom of $A_n A$
$R1$	flow from O
$R2$	flow from $A_n L$
$R3$	flow from $A_n A$
B	tube to account for early lactic acid occurrence
θ, γ, ϕ	tank distances to bottom and top
hydraulic _{2t}	hydraulic two-tank model
Ae	aerobic energy source
An	anaerobic energy sources
p^{Ae}	flow from Ae
p	tap to simulate power output
hydraulic _{weig}	hydraulic model by Weigend et al. (2021b)
AnF	anaerobic fast energy source
AnS	anaerobic slow energy source
m^{Ae}	maximal flow from Ae
m^{AnS}	maximal flow from AnS
m^{AnF}	maximal flow from AnF
U	unlimited energy source
LF	limited fast energy source
LS	limited slow energy source
M_U	maximal flow from U
M_{LF}	maximal flow from LF
M_{LS}	maximal flow from LS

1 Introduction

The quantification of performance (capacity) are a core requirement for optimising training and competition outcomes of an athlete. Performance models are tools for coaches and athletes to obtain such objective quantifications. One of the seminal models in this pursuit is the critical power model (Monod and Scherrer, 1965; Jones et al., 2019). The critical power model uses the parameters critical power (CP) and a finite energy reserve for work above critical power (W'). Physiologically, CP is defined as the threshold between heavy- and severe-intensity exercise (Jones et al., 2019). The capacity W' limits the time an athlete can exercise at a severe intensity above CP. Hill (1993) summarised the assumptions of the critical power model as the following:

1. An individual's power output is a function of two energy sources: aerobic (using oxidative metabolism) and anaerobic (non-oxidative metabolism).
2. Aerobic energy is unlimited in capacity but its conversion rate into power output is limited (CP).
3. Anaerobic energy is limited in capacity but its conversion rate is unlimited.
4. Exhaustion occurs when all of the anaerobic energy capacity is depleted.

Whipp et al. (1982) then denoted the anaerobic energy capacity as W' and both terms were used interchangeably. However, more recent publications suggest that they are not the same (Dekerle et al., 2006). Noordhof et al. (2013) summarised that W' should not be considered as an entirely anaerobic entity and Poole et al. (2016) suggested the conceptualisation of W' as a buffer “to resist exercise intolerance above CP, where the source of the buffer will vary depending on the conditions”.

As already shown by varying definitions for anaerobic energy capacity and W' , all of the above written four assumptions by Hill (1993) are incorrect from a strict physiological point of view (Morton, 2006; Clarke and Skiba, 2013; Poole et al., 2016). Nevertheless, Poole et al. (2016); Jones et al. (2019) described that the elegant abstraction of the critical power model proved to be useful for predicting energy expenditure of an athlete.

Since then, performance models have evolved and a so-called work-balance (W' balance) model has gained increasing popularity due to its intuitive combination of energy expenditure and recovery predictions. Skiba and Clarke (2021) summarised that, even though predictions of W' balance models were of mixed quality, they convince because of their simplicity and their promise of tracking the energy capacities of an athlete in real-time. However, recent findings suggest that current W' balance models overly simplify energy recovery dynamics (Bartram et al., 2018; Caen et al., 2019, 2021). This is also reflected in reviews by Jones and Vanhatalo (2017); Sreedhara et al. (2019); Skiba and Clarke (2021) who highlighted future work on W' balance models to be of great promise for advances in performance modelling.

1.1 A hydraulic analogy

Next to critical power and W' balance models, hydraulic models represent human bioenergetic responses to exercise as liquid flow within a system of pipes and tanks.

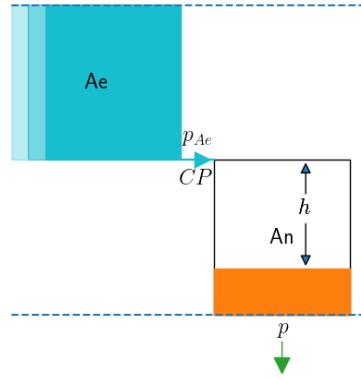


Fig. 1: A hydraulic two-tank model as presented by Morton (2006). The left tank represents the aerobic energy source (Ae) and is of infinite capacity, which is indicated by the fading colour to the left. The right tank represents anaerobic energy sources (An). A pipe (p_{Ae}) connects the bottom of Ae to An and has the maximal flow capacity CP . A tap p is attached to the bottom of An and h indicates the level of depletion of An .

Morton (2006) discussed a hydraulic model with two tanks as an analogy to the assumptions of the critical power model. Henceforth, it will be referred to as the two-tank hydraulic (hydraulic_{2t}) model. A schematic of the hydraulic_{2t} model is depicted in Figure 1.

The first of the above listed assumptions of the critical power model is that power output is a function of two energy sources: aerobic and anaerobic. Each energy source is represented by one tank in Figure 1. The second assumption says that aerobic energy is unlimited. Therefore, the tank Ae is infinite in capacity, indicated by the fading colour to the left. The third assumption is that anaerobic energy is limited in its capacity.

A pipe (p_{Ae}) connects the bottom of the aerobic tank to the anaerobic tank. The flow from this pipe represents sustainable energy contribution because the aerobic tank has infinite capacity. The second assumption states that the conversion of aerobic energy into power output is limited by CP . Therefore, the pipe has the maximal flow capacity CP . At the bottom of the An tank is a tap p . Flow from this tap represents power output.

As discussed above, it is controversial whether W' equates the anaerobic work capacity and, e.g. Sreedhara et al. (2019) avoided this connotation and named the anaerobic tank "Limited capacity" when they described the hydraulic_{2t} model. The present example specifically discusses the hydraulic_{2t} model as an analogy to the above listed assumptions of the critical power model by Hill (1993). Therefore, in this instance, it is justified to interpret the limited tank as anaerobic energy sources with capacity W' . The fill-state of An can drop and rise by h , and the remaining liquid represents available W' balance.

At the beginning of exercise, the anaerobic tank is filled. If power output is below CP , flow from the tap p can be matched by flow from the aerobic tank, and the fill-level of the anaerobic tank does not drop. When power output rises

above CP, maximal flow from the aerobic tank is reached and the liquid level of the anaerobic tank drops by the difference between flow from p and CP at every time step. Exhaustion is reached when the anaerobic tank is depleted. Liquid flow within the example hydraulic_{2t} model resembles the relation of power output, CP, and W' as assumed by the critical power model.

1.2 The M-M model

Next to hydraulic_{2t}, more complex hydraulic models make use of liquid pressure dynamics and make predictions for metabolic responses during exercise with three or four tanks (Morton, 2006; Sundström, 2016). The first hydraulic model was published by Margaria (1976) and later further elaborated by Morton (2006). Morton mathematically defined its dynamics and published it as the Margaria-Morton (M-M) model. An example of the M-M model with the notation of Morton (2006) is depicted in Figure 2. Like Margaria (1976), Morton (2006) labelled the left infinitely big tank as oxidative or aerobic energy source (O). Similarly to Ae of hydraulic_{2t}, the tank O has infinite capacity. The limited tank in the middle represents the anaerobic alactic energy source (A_nA) and the third limited tank on the right represents the anaerobic lactic energy source (A_nL) (Morton, 2006). θ , γ and ϕ define tanks sizes and affect liquid flow dynamics. θ is the distance between the top of A_nA and the top of A_nL . ϕ and γ are the distances between the bottoms of O to A_nL and to A_nA respectively. The pipes R_1 , R_2 , R_3 enable flow between the tanks and have maximal flow capacities.

The depicted situation in Figure 2 is that T has been opened and the fill-level of the middle tank A_nA dropped by h . The more liquid that flows out of the middle tank, the lower the liquid pressures against R_1 , and the more flows from O through R_1 into A_nA . In this way R_1 contributes to the flow out of T . In the situation depicted in Figure 2, T was opened so wide that $h > \theta$ and flow from A_nL began to contribute as well. Its fill-level had dropped by g .

Because the pipe R_1 allows flow from the aerobic source O into the middle tank, Morton (2006) referred to flow through R_1 as \dot{V}_{O_2} . He also defined that the maximal flow through pipe R_1 represents the maximal oxygen uptake ($\dot{V}_{O_2\max}$). Morton (1986) fitted differential equations of his model to collected \dot{V}_{O_2} dynamics and the model could explain the observations well. However, Morton (2006) concluded it had yet to be seen what predictions of the M-M model conform to reality because the model parameters are extremely difficult or impossible to obtain from individual athletes, e.g., θ , γ , ϕ have no direct physiological analogy and the capacities of A_nL and A_nA can only be approximated.

Sundström et al. (2014) investigated predictions of the M-M model in theoretical elaborations. They compared predicted optimal pacing strategies of the M-M model to those of a critical power model for intermittent exercise on an artificial course and reported that the M-M model made more realistic predictions. Sundström (2016) also developed a sophistication of the M-M model and published it as the Margaria-Morton-Sundström (M-M-S) model. However, their work was theoretical, and, like Morton (2006), they also concluded that both their findings and model had yet to be validated on real athlete data.

Lidar et al. (2021) developed an approach to validate the M-M model on real athlete data by fitting parameters to available measurements with an optimisation

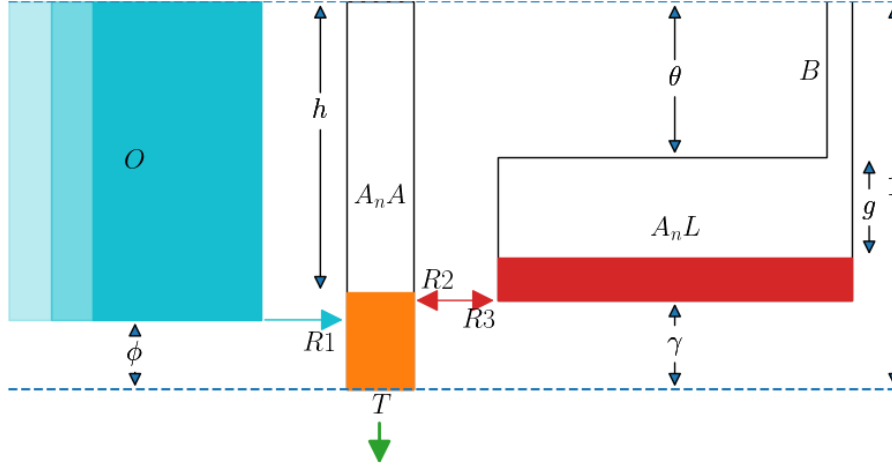


Fig. 2: The M-M model as published by Morton (2006). Hydraulic models approximate human bioenergetic responses to exercise as liquid flow within a system of pipes and tanks. The left infinitely big tank O represents the oxidative or aerobic energy source. The limited tank in the middle (A_nA) represents the alactic anaerobic phosphagens. The right limited tank (A_nL) represents an anaerobic lactic energy source. A tap (T) is attached to A_nA , which can be opened and closed according to energy demand. The tube B accounts for early lactic acid occurrence. The pipes R_1 , R_2 , R_3 enable flow between the tanks. Tank sizes are defined by θ , γ , ϕ .

approach. They fitted two versions of the M-M model and two hydraulic_{2t} models to measured aerobic metabolic rate and accumulated anaerobic energy expenditure during treadmill roller-skiing time trials. Lidar et al. (2021) reported that the hydraulic_{2t} model provided the highest validity and reliability for data it was fitted to and for predictions on unknown data. Further, Lidar et al. (2021) observed that optimal parameters for the fitted M-M model were likely outside the physiologically reasonable ranges and they concluded that the M-M model cannot fully capture bioenergetic responses of the human body to exercise.

1.3 Hydraulic models compared to W' balance models

In Weigend et al. (2021b), we proposed an alternative hydraulic model that, in contrast to Morton (2006); Sundström (2016); Lidar et al. (2021), does not ascribe hydraulic model parameters to alactic or lactic energy sources. The model will henceforth be referred to as hydraulic model by Weigend et al. (2021b) ($\text{hydraulic}_{\text{weig}}$).

$\text{Hydraulic}_{\text{weig}}$ is intended to predict energy expenditure and recovery during high-intensity intermittent exercise in a more general sense. This is reflected in the schematic of $\text{hydraulic}_{\text{weig}}$ depicted in Figure 3. Tube B was removed and the middle tank was re-imagined as general anaerobic fast energy sources (AnF) and the right tank as anaerobic slow energy sources (AnS). These changes removed physiological constraints that Morton (2006); Sundström (2016); Lidar et al. (2021) had

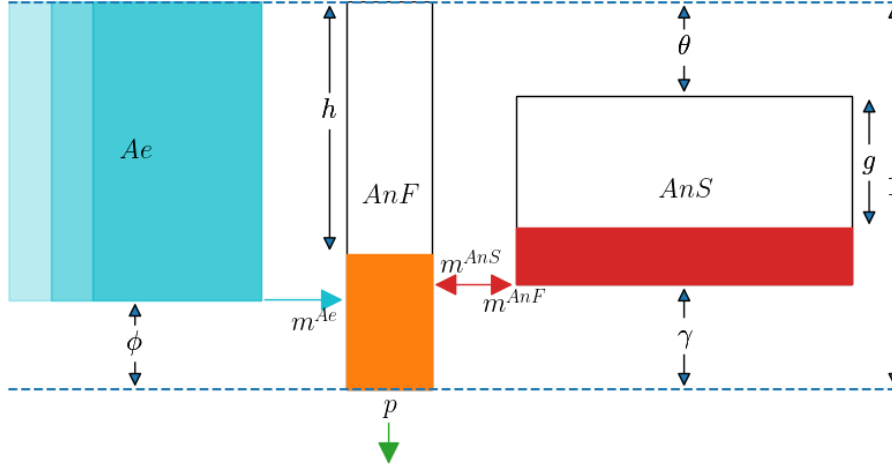


Fig. 3: Representative example of the hydraulic model by $\text{hydraulic}_{\text{weig}}$ as published in Weigend et al. (2021b). In comparison to the M-M model in Figure 2, tube B was removed and the tanks have been renamed as aerobic energy source (Ae), anaerobic fast energy source (AnF) and anaerobic slow energy source (AnS). The maximal flow capacities from tanks are labelled as m^{Ae} , m^{AnS} , m^{AnF} . Tank sizes are defined by θ, γ, ϕ .

to apply to their models and allowed us to adjust and interpret model parameters more freely.

The removal of physiological constraints allowed $\text{hydraulic}_{\text{weig}}$ to serve as an alternative to W' balance models for real-time time-to-exhaustion (TTE) predictions during high-intensity intermittent exercise. Weigend et al. (2021b) proposed a pathway to fit $\text{hydraulic}_{\text{weig}}$ to CP and W' of an athlete. These are the same inputs required by W' balance models. When given these inputs, an evolutionary algorithm fits parameters of $\text{hydraulic}_{\text{weig}}$ such that it predicts TTE during constant high-intensity exercise according to the critical power model, and such that it predicts recovery of W' according to measurements derived from a study by Caen et al. (2019). Specifically, that means the parameters of a fitted $\text{hydraulic}_{\text{weig}}$ model do not directly correspond to CP or W' but the model was fitted to make predictions similar to the critical power model and to published observations for energy recovery.

Therefore, $\text{hydraulic}_{\text{weig}}$ represents a new approach for how hydraulic models can be used. In Weigend et al. (2021a), we retrospectively compared energy recovery predictions of W' balance and $\text{hydraulic}_{\text{weig}}$ models with published data from five studies. The prediction capabilities of $\text{hydraulic}_{\text{weig}}$ outperformed W' balance models on all metrics and rendered it as a strong direction for future research in performance modelling.

However, a remaining similarity between $\text{hydraulic}_{\text{weig}}$ and the M-M model is that the left tank is still labelled as the aerobic energy source. This indicates that the flow from Ae still represents \dot{V}_{O_2} . Because Lidar et al. (2021) recently concluded that the M-M model cannot completely capture the human bioenergetic

system and because the parameters of $\text{hydraulic}_{\text{weig}}$ are fitted without physiological constraints, we hypothesised that flow from Ae of a fitted $\text{hydraulic}_{\text{weig}}$ does not predict realistic \dot{V}_{O_2} dynamics. This had not yet been investigated, and therefore we designed this work to confirm the limitations of $\text{hydraulic}_{\text{weig}}$. Our goal is to support users in interpreting $\text{hydraulic}_{\text{weig}}$ correctly and make users aware of its benefits, but also of its limitations.

2 Methodology

To verify $\text{hydraulic}_{\text{weig}}$ limitations, we compared \dot{V}_{O_2} predictions of $\text{hydraulic}_{\text{weig}}$ to collected \dot{V}_{O_2} data of exercising participants. CP and W' are required to apply $\text{hydraulic}_{\text{weig}}$. These parameters are estimated from TTE performance tests during which participants exercise at constant high intensities until volitional exhaustion. Therefore, we scrutinised $\text{hydraulic}_{\text{weig}}$ \dot{V}_{O_2} predictions on collected data from these TTE tests.

2.1 Data collection

Data collection was approved by the Human Research Ethics Committee at Western Sydney University (HREC Approval Number: H13975). Five recreationally active participants (4 males and 1 female, age 32 ± 7.8 years, weight 73.6 ± 5.81 kg, $\dot{V}_{O_{2\max}} = 3.59 \pm 0.62$ L/min) gave informed and written consent to participate and to have their anonymised data published. All participants were familiar with maximal exercise efforts. Exercise tests were conducted on an SRM - High Performance Ergometer (Jülich, Germany) in hyperbolic operation mode, which adjusts power dynamically to cadence changes to maintain a constant power output. Breath-by-breath \dot{V}_{O_2} data was collected using the Quark CPET system by COSMED (Rome, Italy). The equipment was calibrated prior to each trial. Each of the 5 participants completed 6 exhaustive exercise trials. To ensure that participants were fully rested, they were asked to avoid strenuous exercise 24 h prior the tests and tests were scheduled more than 24 h apart, roughly at the same time of the day.

2.1.1 Ramp test

All participants had to perform an initial ramp test to obtain the appropriate power settings for subsequent TTE tests. After a 3-min warm-up at 50 W, the power increased by 30 W per min for males and by 20 W per min for the female. Once power rose above 110 W, participants were instructed to maintain a self-chosen cadence between 80-100 RPM. The point of volitional exhaustion was defined as the first time point when the cadence dropped by more than 10% below the intended cadence for more than 3 s. The highest 10-s moving average power output achieved was defined as the peak power output (P_{peak}).

2.1.2 TTE tests

After the ramp test, each participant completed 5 constant power TTE trials at distinct powers in random order. The powers were set to 100%, 92.5%, 85%, 80% and 77.5% or 75% of P_{peak} to obtain a range of TTEs between 2 min and 12 min. Participants were blinded to their exercise power. Again, each test started with a 3-min warm-up at 50 W before power was set to the randomly chosen percentage of P_{peak} . During exercise, participants were asked to cycle at their self-chosen cadence from the ramp test and the point of volitional fatigue was defined as the first time point when cadence dropped by more than 10% below the intended cadence for more than 3 s. Throughout all tests, breath-by-breath \dot{V}_{O_2} data was collected. For each test, the highest achieved 30-s moving average of measured \dot{V}_{O_2} was considered as the peak oxygen uptake ($\dot{V}_{\text{O}_{2\text{peak}}}$) of that test. TTEs as well as power-meter data of the SRM ergometer were also recorded for later analysis.

2.2 Data analysis

Weigend et al. (2021b) designed $\text{hydraulic}_{\text{weig}}$ to serve as an alternative to W' balance models and—like W' balance models— $\text{hydraulic}_{\text{weig}}$ requires CP and W' to make predictions. These parameters were obtained by fitting the critical power model to conducted TTE tests of a participant.

2.2.1 Fitting the models

To obtain CP and W' that best fit a participant, three forms of the critical power model were fitted to conducted TTE tests. These forms were

$$TTE = \frac{W'}{P - CP}, \quad (1)$$

which will be henceforth referred to as the nonlinear power-time model,

$$P \cdot TTE = CP \cdot TTE + W', \quad (2)$$

which will be henceforth referred to as the linear work-time model, and

$$P = W' \cdot \frac{1}{TTE} + CP, \quad (3)$$

which will be henceforth referred to as the linear power-1/time model (Hill, 1993).

The goodness of fit of each model was determined from the standard error of estimation (SEE) associated with fitted CP and W' . The goodness of fit of a model was considered sufficient if SEE associated with CP was $< 5\%$ of CP and the SEE associated with W' was $< 10\%$ of W' (Jones et al., 2019; Caen et al., 2021). The best individual fit for a participant was selected by which model resulted in the smallest sum of the SEE associated with CP as % of CP plus the SEE associated with W' as % of W' (Black et al., 2015; Jones et al., 2019; Caen et al., 2021).

Then, $\text{hydraulic}_{\text{weig}}$ was fitted to the derived CP and W' with the procedure published in Weigend et al. (2021b). Considering the notation in Figure 3, fitting $\text{hydraulic}_{\text{weig}}$ meant finding a set of parameters for $[AnF, AnS, m^{Ae}, m^{AnS}]$,

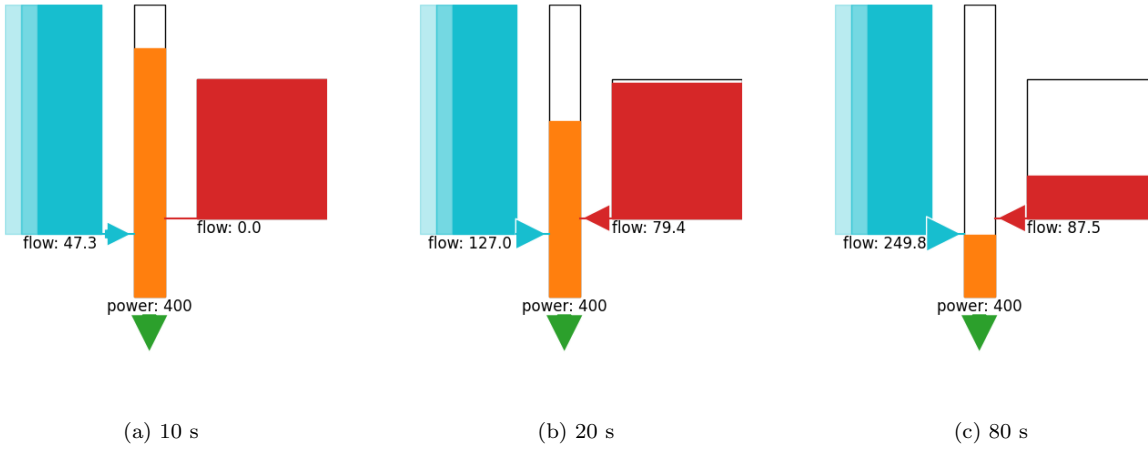


Fig. 4: Snapshots of a $\text{hydraulic}_{\text{weig}}$ model simulating exercise at a constant intensity of 400 W. Depicted are fill-levels of tanks and the flows between them after 10, 20, and 80 s.

$m^{AnF}, \theta, \gamma, \phi]$ that made the hydraulic model resemble expected exercise responses according to the critical power model for energy expenditure, and according to published recovery ratios for energy recovery (Caen et al., 2019; Weigend et al., 2021b). To find these parameters for our participants, we used the automatised evolutionary computation procedure of our `threecomphyd`¹ Python package, which was published in Weigend et al. (2021b).

2.2.2 \dot{V}_{O_2} predictions

To assess the quality of predicted \dot{V}_{O_2} kinetics of fitted $\text{hydraulic}_{\text{weig}}$ models, the predictions were compared to the collected breath-by-breath \dot{V}_{O_2} data of the TTE tests. To elaborate how \dot{V}_{O_2} predictions were computed, we use the example in Figure 4, which displays snapshots of a $\text{hydraulic}_{\text{weig}}$ model that simulates an exercise with constant intensity.

At the beginning of exercise at second 0, all tanks were filled. When exercise started, the tap at the bottom of the middle tank was opened according to the energy demand. Liquid flowed out, and the fill-level of the middle tank dropped accordingly. As a consequence, liquid pressure against the pipe exit of the left tank dropped and thus the liquid flow from the left tank increased.

In the example in Figure 4, the tap was opened according to 400 W and after 10 s, the fill-level of the middle tank dropped halfway to the top of the right tank. Flow from the left tank increased to an equivalent of 47.3 W. As observable in the snapshot at 20 s, when the fill-level of the middle tank dropped below the top of the right tank, liquid from the right tank also flowed into the middle tank. In the snapshot at 80 s, the fill-level of the middle tank dropped below the exit of

¹ https://github.com/faweigend/three_comp_hyd

the pipe of the left tank, and thus the flow from the left tank was at maximum capacity m^{Ae} .

According to the definitions of Morton (2006), the left tank represents the aerobic contribution, and therefore the flow from the left tank represents oxygen uptake (\dot{V}_{O_2}). With this understanding, we opened and closed the tap according to collected SRM power-meter data and recorded flow from the left tank as predicted \dot{V}_{O_2} kinetics. We compared \dot{V}_{O_2} predictions with collected breath-by-breath data from all constant power TTE trials.

Our objective measure to assess the quality of \dot{V}_{O_2} predictions was the difference between the time at which the simulated flow from the left tank (Ae) was predicted to reach its peak, and the time at which the observed breath-by-breath \dot{V}_{O_2} data reached $\dot{V}_{O_{2peak}}$. As an additional visual comparison, we plotted normalised predicted flow from Ae together with normalised actual \dot{V}_{O_2} dynamics. Predicted \dot{V}_{O_2} dynamics (flow from Ae) were normalised with the maximal flow m^{Ae} . The 30 s averaged real \dot{V}_{O_2} uptake measurements were normalised with the observed $\dot{V}_{O_{2peak}}$ during that test.

3 Results

3.1 Ramp test results and model fittings

The average P_{peak} of the ramp tests of all participants was 327 ± 52 W. The shortest TTE was excluded from the estimation of CP and W' for one participant because it was too short (113 s). For all participants, the linear power-1/time model resulted in the best individual fit and resulted in an averaged CP of 223 ± 40 W and W' of 148912 ± 2869 J. Individual critical power model fitting results and associated SEEs are summarised in Table A1 in the Appendix.

Using the notation of Figure 3, the fitted hydraulic_{weig} models had an average AnF of 14330 ± 2463 J, AnS of 38575 ± 6605 J, m^{Ae} of 222 ± 40 W, m^{AnS} of 90 ± 15 W, θ of 0.7 ± 0.05 , γ of 0.02 ± 0.01 , and ϕ of 0.26 ± 0.04 . Individual results for these parameters are summarised in Table A2 in the Appendix.

3.2 \dot{V}_{O_2} predictions

Of all 25 constant power tests, the tests of participant 4 at 288 W and participant 5 at 255 W were excluded from the \dot{V}_{O_2} analysis. In these two cases, unrealistic drops in \dot{V}_{O_2} indicated that the breathing mask was not fixed tight enough and leaked air when participants lowered their head too far. The unrealistic drops are clearly recognisable and depicted in Figures A1 and A2 in the Appendix.

The defined objective measure to assess the quality of \dot{V}_{O_2} predictions was the time difference between predicted and observed $\dot{V}_{O_{2peak}}$. Furthermore, normalised flow from Ae and measured breath-by-breath data were plotted for visual comparison. An example for such a plot is depicted in Figure 5. The power output measured by the SRM power-meter is plotted as the grey area in the background. It is overlaid with predicted and observed \dot{V}_{O_2} kinetics. The time at which hydraulic_{weig} predicted $\dot{V}_{O_{2peak}}$ was 63 s after the commencement of exercise. The time at which the actual $\dot{V}_{O_{2peak}}$ was observed was 258 s after the commencement of exercise.

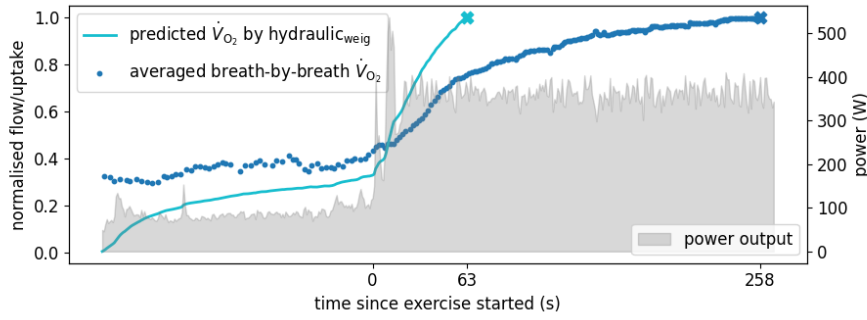


Fig. 5: Measured power-meter output and \dot{V}_{O_2} of participant 2 during warm-up and a TTE test at 364 W. Measurements before second 0 are part of the 3-min warm-up at 50 W. The plotted line displays predicted \dot{V}_{O_2} uptake (flow from Ae) of a hydraulic_{weig} model fitted to CP and W' of participant 2. The averaged collected breath-by-breath \dot{V}_{O_2} data is depicted as dots. The x-symbols mark the time points when hydraulic_{weig} predicted $\dot{V}_{O_{2peak}}$ (63 s) and when collected averaged breath-by-breath reached $\dot{V}_{O_{2peak}}$ (258 s). The prediction error was 195 s.

Therefore, the prediction error was 195 s. In addition, it is observable that the predicted \dot{V}_{O_2} started at 0 and increased slowly during the warm-up.

The example Figure 5 is representative for all tests. As summarised in Table 1, on average, $\dot{V}_{O_{2peak}}$ was observed after 282 ± 134 s of exercise, while hydraulic_{weig} predicted $\dot{V}_{O_{2peak}}$ after 65 ± 24 s of exercise in the respective test. In all the tests investigated, hydraulic_{weig} predicted a much faster rise in \dot{V}_{O_2} and a too early $\dot{V}_{O_{2peak}}$ with an average prediction error of 216 ± 113 s. Table 1 summarises our results. The best hydraulic_{weig} prediction was 67 s too early. The worst prediction was 461 s too early. The prediction error decreased as the exercise power increased.

4 Discussion

Previously, theoretical hydraulic performance models of Morton (2006) and Sundström (2016) promised predictions for metabolic responses during exercise, e.g., for lactic, alictic, and aerobic energy sources. But their models were not suitable for real-world applications because the required parameters to apply these models, e.g., precise lactic energy capacities in Joules, were impossible to obtain from individual athletes. Lidar et al. (2021) fitted parameters for the M-M model to available measurements and concluded that it likely cannot fully capture the human bioenergetic system.

In Weigend et al. (2021b), we presented a more abstract hydraulic model that represented a different pathway for how hydraulic models can be used. Hydraulic_{weig} was designed to serve as an alternative to W' balance models for TTE predictions during intermittent exercise. To be comparable to W' balance models Weigend et al. (2021b) proposed a pathway to obtain hydraulic_{weig} predictions from CP and W' . We observed in Weigend et al. (2021a) that hydraulic energy recovery

Table 1: The summary of hydraulic_{weig} prediction errors for $\dot{V}_{O_{2peak}}$. The example from Figure 5 (participant 2 with 364 W) is in row 8. The column “observed” informs about the seconds it took from the onset of exercise to reach $\dot{V}_{O_{2peak}}$ (blue x-symbol at 258 s in Figure 5). The column “predicted” informs about the seconds hydraulic_{weig} predicted it would take (azure x-symbol at 63 s in Figure 5). The prediction error in the last column is the difference between these two times.

participant	power (W)	time until $\dot{V}_{O_{2peak}}$ (s)		prediction error (s)
		observed	predicted	
1	243	481	72	409
1	259	230	53	177
1	275	196	45	151
1	299	156	41	115
1	324	120	34	86
2	332	484	88	396
2	343	297	78	219
2	364	258	63	195
2	396	169	54	115
2	428	137	44	93
3	252	479	113	366
3	265	355	85	270
3	280	230	72	158
3	307	154	53	101
3	330	109	42	67
4	224	581	120	461
4	230	445	94	351
4	245	330	85	245
4	265	266	67	199
5	214	309	68	241
5	221	292	55	237
5	234	249	44	205
5	276	152	32	120
avg±std		282±134	65±24	216±113

predictions outperformed energy recovery predictions by W' balance models and our findings marked hydraulic models as a strong direction for future research in performance modelling.

Hydraulic_{weig} is a more general interpretation of the M-M model. We hypothesised that, although the parameters of the hydraulic_{weig} model have an aerobic and anaerobic connotation, it cannot make realistic predictions for \dot{V}_{O_2} . Hydraulic_{weig} was designed to predict TTEs during intermittent exercise, but because its tanks and pipes resemble the M-M model so closely, it is tempting to interpret hydraulic_{weig} in a metabolic context. In the present study, we confirmed, with data collected from 23 performance tests of 5 participants, that hydraulic_{weig} is not suitable for \dot{V}_{O_2} predictions.

4.1 Predictions of \dot{V}_{O_2} slow component

From the onset of high-intensity exercise, $\text{hydraulic}_{\text{weig}}$ consistently predicted \dot{V}_{O_2} to rise too fast. As summarised in Table 1, \dot{V}_{O_2} was predicted to reach its peak after an average of 65 ± 24 s while observed kinetics were slower and took 282 ± 134 . The average difference between $\dot{V}_{O_{2\text{peak}}}$ predictions and observations was 216 ± 113 s. Considering that TTE tests lasted between 2-12 min, prediction errors of more than 3 min on average made clear that $\text{hydraulic}_{\text{weig}}$ could not predict realistic \dot{V}_{O_2} kinetics.

Further, it is observable in Table 1 that the prediction error increases with decreasing power. Thus, the longer the exercise, the larger the error in predicted \dot{V}_{O_2} . These results are in contrast to remarks by Morton (2006) for \dot{V}_{O_2} prediction capabilities of his M-M model and we elaborate the reasons for such poor predictions in the following. We begin by summarising the physiological constraints that Morton (2006) applied to his M-M model.

4.1.1 M-M model and \dot{V}_{O_2} slow component

Looking at the M-M model, tank positions are determined by the values θ, γ and ϕ . Because each tank represents a concrete bioenergetic energy source, Morton (1986, 1990, 2006) developed several constraints on θ, γ and ϕ to find a realistic arrangement of tanks for his model:

- Pipe R_2/R_3 has to be above R_1 ($\gamma > \phi$) because athletes can deplete their glycogen stores when exercising below $\dot{V}_{O_{2\text{max}}}$.
- The onset of flow through R_2 represents the lactate threshold (moderate-heavy boundary) (LAT), i.e., the commencement of increased lactic acid production. Therefore, the top of tank $A_n A$ has to have some distance to the top of the entire system ($\theta > 0$) and should be at approximately 40% of the height of O .
- During constant severe intensity exercise, \dot{V}_{O_2} rises asymptotic to a maximal value. When exercise stops, oxygen consumption does not decline immediately. Therefore, R_1 cannot be at the top or bottom of the middle tank ($0 < \phi < 1$).

From these constraints, Morton (1990) argued that the only realistic configuration of the three component hydraulic model is the one depicted in Figure 2.

In his review, Morton (2006) particularly highlighted how the M-M model predicts the \dot{V}_{O_2} slow component phenomenon. Barstow and Mole (1991) empirically showed that \dot{V}_{O_2} uptake quickly reaches a steady state at a constant exercise intensity below LAT. However, at exercise above LAT an initial rapid increase in \dot{V}_{O_2} uptake is followed by a slower continuous rise. This slower rise is called the \dot{V}_{O_2} slow component.

As observable in Figure 6, the slow component is well captured by a hydraulic model that is configured according to the above stated constraints on the M-M model. Depicted on the right in Figure 6 are the predicted \dot{V}_{O_2} dynamics (flow from A_e) during constant high intensity exercise. With all tanks filled at the beginning, the dynamics play out as follows: During the warm-up, the tap was not opened wide and thus liquid level in the middle tank drops slowly and flow from A_e increases slowly. Then exercise starts after one min, the fill-level in the middle tank drops quickly and therefore flow from A_e increases quickly. The exercise intensity is high

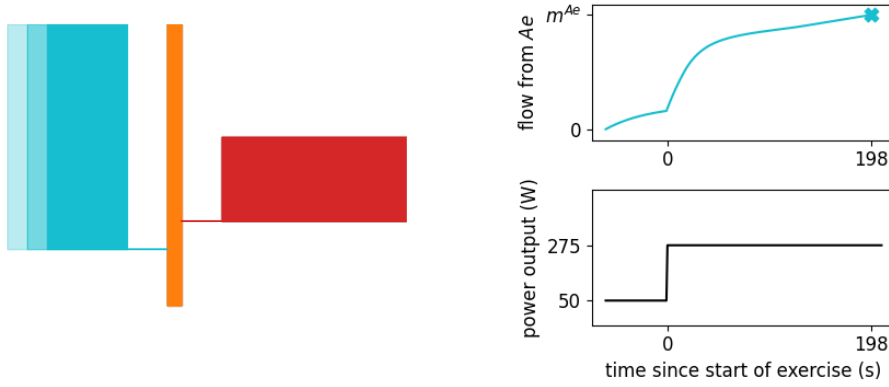


Fig. 6: Left: A hydraulic_{weig} model configured in a way that follows the physiological constraints on the M-M model discussed in Section 4.1.1. Right: The top plot displays flow from the left tank (Ae) into the middle tank (AnF). The displayed model simulates constant intensity exercise at 275 W with a warm-up at 50 W until maximal flow through Ae is reached (x-symbol). We interpreted this flow as \dot{V}_{O_2} uptake predictions. The \dot{V}_{O_2} slow component is observable in predicted \dot{V}_{O_2} dynamics.

enough, so that the dropping fill-level of the middle tank reaches the top of the right tank, the right tank also starts to contribute. This additional flow makes the fill-level of the middle tank drop slower and therefore, flow from Ae increases slower from this point. Morton (2006) stated that the way in which the M-M model simulates the \dot{V}_{O_2} slow component can be compared to the mathematical formulation by Barstow and Mole (1991).

4.1.2 Hydraulic_{weig} and the \dot{V}_{O_2} slow component

Due to our fitting procedure that adjusts hydraulic model parameters freely, it is not guaranteed that hydraulic_{weig} conforms to the above discussed constraints on the M-M model. As reported in our results in Section 3, the average parameter γ of the fitted hydraulic_{weig} was 0.017 ± 0.005 and the average ϕ was 0.263 ± 0.038 . These values indicate that none of the hydraulic_{weig} models adhered the constraint of Morton (1990) that $\gamma > \phi$. This had a direct impact on \dot{V}_{O_2} predictions of hydraulic_{weig}. As an example, on the left in Figure 7 is the system of tanks fitted to participant 1. Here, the parameters are $\gamma = 0.02$ and $\phi = 0.27$, so $\gamma < \phi$. In addition, the top of the right tank is much lower than the tank of the model depicted in Figure 6. The second constraint of Morton (1990) suggests that the top of AnS to be at approximately 40% of the height of Ae , which is also not satisfied with the fitted model in Figure 7. As a result, \dot{V}_{O_2} predictions of the model fitted to participant 1 did not resemble the \dot{V}_{O_2} slow component. The onset of flow from the right tank had almost no impact on the exponential increase of flow from the left tank. This explains the prediction errors in Table 1 and confirms on the example

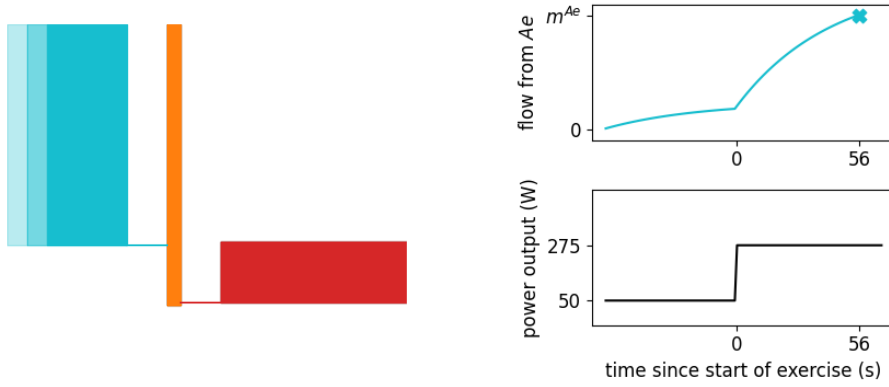


Fig. 7: Left: A three component hydraulic model fitted to CP 211 W and W' 13240 J of participant 1. Values of all fitted parameters are in Table A2 in the Appendix. Right: Flow from Ae when the left model simulates a warm-up at 50 W and then a constant high intensity exercise at 275 W until maximal flow through Ae is reached (x-symbol).

of \dot{V}_{O_2} predictions that the hydraulic_{weig} model allows for unrealistic predictions for metabolic responses during exercise.

4.2 Warm-up \dot{V}_{O_2} predictions

Another example of unrealistic \dot{V}_{O_2} predictions occurs at the beginning of exercise during the warm-up. Because the middle tank of hydraulic_{weig} is filled initially, it will always predict the complete absence of \dot{V}_{O_2} at the first time step of a simulation. As observable in Figures 5 to 7, this caused unrealistic \dot{V}_{O_2} predictions at the beginning of exercise tests. Predicted \dot{V}_{O_2} started at 0 and increased slowly throughout the 3 min of warm-up at 50 W. The size of the middle tank is fixed for the M-M and hydraulic_{weig} models. Therefore, if the flow from Ae is interpreted as \dot{V}_{O_2} , these models are guaranteed to predict the absence of \dot{V}_{O_2} at the beginning of exercise and when the athlete is fully recovered.

Lidar et al. (2021) acknowledged this issue and introduced a new parameter to shrink the size of the middle tank. Using the notation in Figure 3, Lidar et al. (2021) made the top of AnF adjustable and introduced a parameter ψ , which defines the distance between the top of AnF and the top of Ae . The closer ψ to $1 - \phi$, the larger the flow from Ae at the start of the simulation. This additional parameter is not present in the M-M or hydraulic_{weig} models and is another argument for why hydraulic_{weig} cannot make realistic predictions for \dot{V}_{O_2} .

4.3 New labels for hydraulic_{weig}

When the hydraulic_{weig} model was first proposed in Weigend et al. (2021b), we chose to name the left infinitely big tank the aerobic energy source (Ae) and

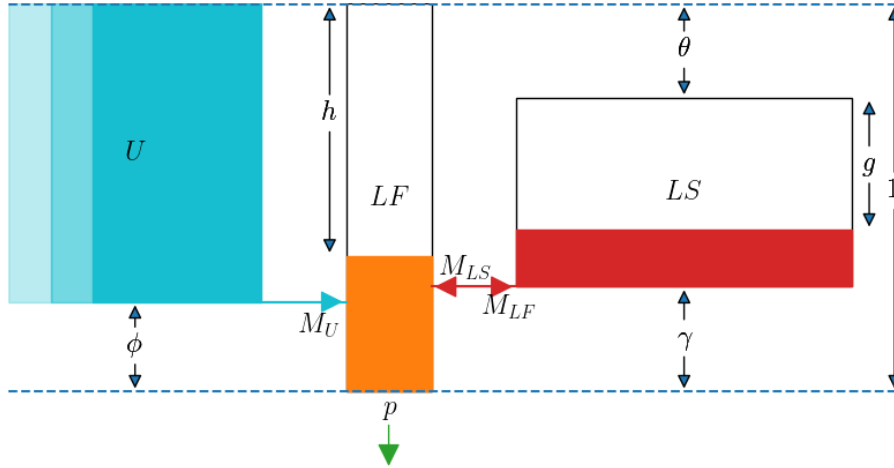


Fig. 8: We assigned new labels to our three component hydraulic model $\text{hydraulic}_{\text{weig}}$. Tanks are named unlimited energy source U , limited fast energy source (LF), limited slow energy source (LS). Maximal flow capacities from these tanks are named M_U , M_{LS} , and M_{LF} .

the two limited tanks the anaerobic fast (AnF) and anaerobic slow energy source (AnS). These names have a bioenergetic connotation and imply that the flow from the aerobic source still represents \dot{V}_{O_2} uptake like it did in the M-M model and the model of Margaria (1976). The results of this work show that $\text{hydraulic}_{\text{weig}}$ does not predict realistic \dot{V}_{O_2} dynamics and should not be used for \dot{V}_{O_2} predictions.

Therefore, it is a sensible clarification to change the labels of $\text{hydraulic}_{\text{weig}}$ to more abstract names. The model with all new labels is depicted in Figure 8. Instead of Ae , we re-labelled the left tank as an unlimited energy source (U). Instead of AnF , the middle tank is now a limited fast energy source (LF), and instead of AnS , the right tank is a limited slow energy source (LS). These changes do not apply to any other hydraulic models and only affect $\text{hydraulic}_{\text{weig}}$. They are an important step to protect users from misinterpreting fitted $\text{hydraulic}_{\text{weig}}$ models and their prediction results.

5 Future work

The above discussion recommends sensible directions for future work to broaden the range of possible applications for fitted three tank hydraulic models. Unrealistic \dot{V}_{O_2} predictions during high-intensity constant exercise can be improved by forcing a fitting approach to adhere to the previously discussed constraints of the M-M model. Lidar et al. (2021) did not consider these constraints and their fitted hydraulic models violated the same constraint that $\text{hydraulic}_{\text{weig}}$ violated in this work (in their Table 3 the λ parameter of their model is smaller than ϕ). Incorporating these constraints will considerably complicate the fitting procedures. Nevertheless, this could be a worthwhile direction for future research investigating

if predictions of fitted three tank hydraulic models for metabolic responses during exercise can be improved.

However, the current focus and strength of $\text{hydraulic}_{\text{weig}}$ are energy recovery predictions during intermittent exercise, where promising new investigation opportunities emerge. Platforms like Strava² or Golden Cheetah³ provide constantly growing databases of real-world intermittent exercise training and competition data. With affordable power metres, smartwatches, and online cycling apps such as Zwift⁴, the interest in intermittent exercise performance models and the amount of available data will grow. The future holds exciting possibilities for new iterations of W' balance or hydraulic models, and the earlier we begin to develop pathways to investigate these models on such real-world data, the better. Therefore, while future work to apply hydraulic models to metabolic predictions and other modes of exercise is important, it is equally important to foster and develop its real-world application in intermittent exercise.

6 Conclusion

As already summarised by Morton (2006) for bioenergetic models or by Skiba and Clarke (2021) for W' balance models, one-size-fits-all performance models do not exist. For simplicity, let us imagine a spectrum where simple and applicable performance models are on the left and complex and theoretical models are on the right. One could say that the critical power model is on the far left because it has only two parameters and requires just a few performance tests to be applied. Then, the hydraulic models of Morton (2006); Lidar et al. (2021) and Sundström (2016) would be on the right because they have eight or more parameters and could not be applied to athletes due to the required in-depth knowledge about bioenergetic capacities. We showed that our $\text{hydraulic}_{\text{weig}}$ bridges the gap and remains somewhere in the middle. It can be applied to athletes and outperforms W' balance models in intermittent exercise predictions. However, it should not be used for predictions of \dot{V}_{O_2} or alactic or lactic energy sources as the original hydraulic models were intended to be used.

Depending on focus and setup, users must make well-informed decisions which of the available performance models are suitable for their analysis. This work further contributed to positioning our $\text{hydraulic}_{\text{weig}}$ model with its advantages and limitations among other existing performance models. We strive to promote progress in performance model development and to help users to make informed decisions for their analysis. As outlined in future work, there is an abundance of directions for creating new models and improving existing ones. To support this pursuit, we introduced new labels for our model. Furthermore, we embedded all our data, code of compared models, and hydraulic model advances in the open-source python packages `pypermod`⁵ and `threecomp_hyd`⁶.

² <https://www.strava.com>

³ <https://www.goldencheetah.org>

⁴ <https://www.zwift.com>

⁵ <https://github.com/faweigend/pypermod>

⁶ https://github.com/faweigend/three_comp_hyd

7 Statements and Declarations

Funding No funding was received to assist with the preparation of this manuscript.

Competing interests The authors have no competing interests to declare that are relevant to the content of this article.

Author contribution statement FCW and JS and OO and EG conceived and designed research. FCW conducted data collection. FCW analysed the data. FCW and EG wrote the manuscript. All authors read and approved the manuscript.

Data and code availability Most relevant measurements on participants are summarised in the Appendix. Further, the datasets generated during the current study and the code for its analysis are available in the `pypermod` repository, <https://github.com/faweigend/pypermod>

References

- Barstow, T. J. and Mole, P. A. (1991). Linear and nonlinear characteristics of oxygen uptake kinetics during heavy exercise. *Journal of Applied Physiology*, 71(6):2099–2106.
- Bartram, J. C., Thewlis, D., Martin, D. T., and Norton, K. I. (2018). Accuracy of W' recovery kinetics in high performance cyclists - modeling intermittent work capacity. *International Journal of Sports Physiology and Performance*, 13(6):724–728.
- Black, M. I., Jones, A. M., Bailey, S. J., and Vanhatalo, A. (2015). Self-pacing increases critical power and improves performance during severe-intensity exercise. *Applied Physiology, Nutrition, and Metabolism*, 40(7):662–670.
- Caen, K., Bourgois, G., Dauwe, C., Blancquaert, L., Vermeire, K., Lievens, E., Van Dorpe, J., Derave, W., Bourgois, J. G., Pringels, L., and Boone, J. (2021). W' Recovery Kinetics following Exhaustion: A Two-Phase Exponential Process Influenced by Aerobic Fitness. *Medicine & Science in Sports & Exercise*, Publish Ahead of Print.
- Caen, K., Bourgois, J. G., Bourgois, G., Van Der Stede, T., Vermeire, K., and Boone, J. (2019). The reconstitution of W' depends on both work and recovery characteristics. *Medicine & Science in Sports & Exercise*, 51(8):1745–1751.
- Clarke, D. C. and Skiba, P. F. (2013). Rationale and resources for teaching the mathematical modeling of athletic training and performance. *Advances in Physiology Education*, 37(2):134–152.
- Dekerle, J., Brickley, G., Hammond, A. J. P., Pringle, J. S. M., and Carter, H. (2006). Validity of the two-parameter model in estimating the anaerobic work capacity. *European Journal of Applied Physiology*, 96(3):257–264.
- Hill, D. W. (1993). The critical power concept: a review. *Sports Medicine*, 16(4):237–254.
- Jones, A. M., Burnley, M., Black, M. I., Poole, D. C., and Vanhatalo, A. (2019). The maximal metabolic steady state: redefining the 'gold standard'. *Physiological Reports*, 7(10):e14098.
- Jones, A. M. and Vanhatalo, A. (2017). The 'critical power' concept: applications to sports performance with a focus on intermittent high-intensity exercise. *Sports Medicine*, 47(S1):65–78.
- Lidar, J., Andersson, E. P., and Sundström, D. (2021). Validity and Reliability of Hydraulic-Analogy Bioenergetic Models in Sprint Roller Skiing. *Frontiers in Physiology*, 12:726414.
- Margaria, R. (1976). *Biomechanics and energetics of muscular exercise*. Oxford University Press, Oxford University Press, Walton Street, Oxford, OX2 6DP.
- Monod, H. and Scherrer, J. (1965). The work capacity of a synergetic muscular group. *Ergonomics*, 8(3):329–338.
- Morton, R. H. (1986). A three component model of human bioenergetics. *Journal of Mathematical Biology*, 24(4):451–466.
- Morton, R. H. (1990). Modelling human power and endurance. *Journal of Mathematical Biology*, 28(1):49–64.
- Morton, R. H. (2006). The critical power and related whole-body bioenergetic models. *European Journal of Applied Physiology*, 96(4):339–354.
- Noordhof, D. A., Skiba, P. F., and de Koning, J. J. (2013). Determining anaerobic capacity in sporting activities. *International Journal of Sports Physiology and*

- Performance*, 8(5):475–482.
- Poole, D. C., Burnley, M., Vanhatalo, A., Rossiter, H. B., and Jones, A. M. (2016). Critical power: an important fatigue threshold in exercise physiology. *Medicine & Science in Sports & Exercise*, 48(11):2320–2334.
- Skiba, P. F. and Clarke, D. C. (2021). The W’ Balance Model: Mathematical and Methodological Considerations. *International Journal of Sports Physiology and Performance*, 16(11):1561–1572.
- Sreedhara, V. S. M., Mocko, G. M., and Hutchison, R. E. (2019). A survey of mathematical models of human performance using power and energy. *Sports Medicine - Open*, 5(1):54.
- Sundström, D. (2016). On a bioenergetic four-compartment model for human exercise. *Sports Engineering*, 19(4):251–263.
- Sundström, D., Carlsson, P., and Tinnsten, M. (2014). Comparing bioenergetic models for the optimisation of pacing strategy in road cycling. *Sports Engineering*, 17(4):207–215.
- Weigend, F. C., Clarke, D. C., Obst, O., and Siegler, J. (2021a). A hydraulic model outperforms work-balance models for predicting recovery kinetics from intermittent exercise. *arXiv:2108.04510 [cs]*. arXiv: 2108.04510.
- Weigend, F. C., Siegler, J., and Obst, O. (2021b). A new pathway to approximate energy expenditure and recovery of an athlete. In *Proceedings of the Genetic and Evolutionary Computation Conference Companion*, pages 325–326, Lille France. ACM.
- Whipp, B. J., Huntsman, D. J., Storer, T. W., Lamarra, N., and Wasserman, K. (1982). A constant which determines the duration of tolerance to high-intensity work. *Federation proceedings*, 41(5):1591–1591.

A Appendix

Table A1: An overview of critical power model fitting results for all participants. SEE% denotes the standard error associated with the parameter as a percentage of the parameter, e.g, SEE% of CP is the SEE associated with CP divided by CP.

participant	best fit model	CP		W'	
		W	SEE%	J	SEE%
1	linear power-1/time	211	3.1	13240	8.7
2	linear power-1/time	292	2.4	19143	8.0
3	linear power-1/time	238	0.7	10820	3.6
4	linear power-1/time	199	1.8	16790	6.3
5	linear power-1/time	174	1.5	14469	3.8
avg \pm std		223 \pm 40	1.9 \pm 0.8	14892 \pm 2869	6.1 \pm 2.1

Table A2: An overview of parameters of fitted hydraulic_{weig} models.

participant	AnF (J)	AnS (J)	m^{Ae} (W)	m^{AnS} (W)	m^{AnF} (W)	θ	γ	ϕ
1	12562	36679	210	82	14	0.71	0.02	0.27
2	18245	50537	291	117	20	0.7	0.02	0.27
3	11914	38269	238	71	11	0.79	0.02	0.2
4	16196	37141	198	95	15	0.68	0.01	0.27
5	12733	30250	173	87	14	0.64	0.02	0.31
avg \pm std	14330 \pm 2463	38575 \pm 6605	222 \pm 40	90 \pm 15	15 \pm 3	0.7 \pm 0.05	0.02 \pm 0.01	0.26 \pm 0.04

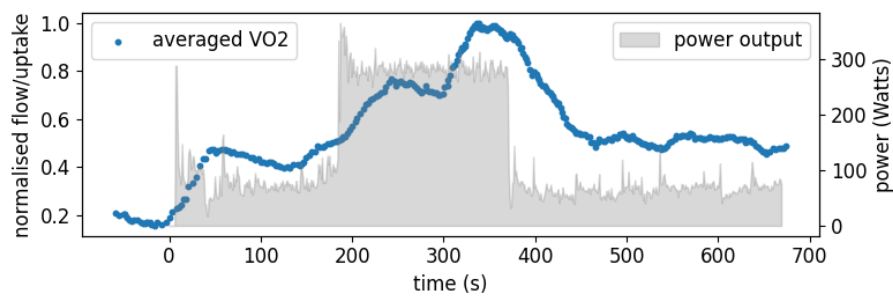


Fig. A1: Measured power output (grey area) and \dot{V}_{O_2} uptake (dots) of participant 4 during a constant intensity exercise trial at 288 W. \dot{V}_{O_2} drops occurred because the face mask leaked air when the athlete lowered their head too far.

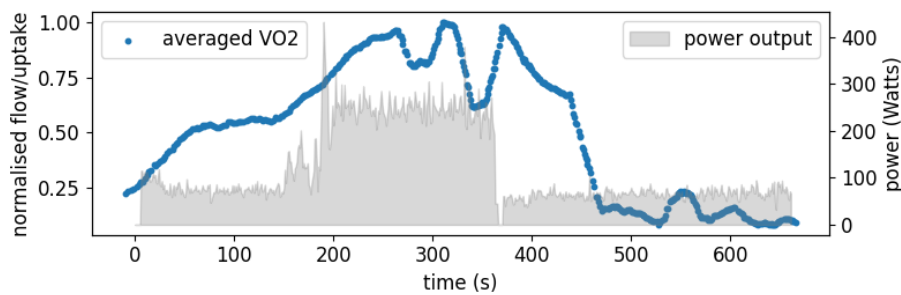


Fig. A2: Measured power output (grey area) and \dot{V}_{O_2} uptake (dots) of participant 5 during a constant intensity exercise trial at 255 W. \dot{V}_{O_2} drops occurred because the face mask leaked air when the athlete lowered their head too far.